Black carbon radiative heating effects on cloud microphysics and implications for the aerosol indirect effect: 2. Cloud microphysics

Athanasios Nenes, William C. Conant and John H. Seinfeld

Departments of Chemical Engineering and Environmental Science and Engineering, Mail Code 210-41, California Institute of Technology, Pasadena, California, 91125, USA

Abstract. This work examines the effect of black carbon (BC) radiative heating on cloud droplet formation. Changes in cloud droplet concentration and cloud albedo due to the presence of black carbon are computed for different cases of aerosol size distributions, meteorological conditions, BC mixing state, and aerosol composition. We examine the effect of three new mechanisms (that result from BC heating) that can affect cloud droplet number and lifetime. Two of these mechanisms act to *increase* cloud droplet number or lifetime: *i*) the ability of BC to decrease the collection efficiency of giant CCN, and, *ii*) the delayed growth of low S_c CCN that allow higher S_c CCN to form droplets. These two mechanisms complement each other in terms of increasing cloud droplet number, since it is shown that the former is most efficient at strong updrafts, and the latter at low updraft velocities. A third mechanism identified, gas-phase heating (which is different from the so-called "semi-direct effect") in our simulations acts to decrease LWC, and thus albedo; however the droplet number concentration does not change significantly due to dynamic readjustments in cloud supersaturation. The simulations indicate that the mixing state of BC with the CCN population can have an important influence on the effect of BC heating on the droplet population. Although additional work is necessary to fully assess the effects of BC heating on cloud microphysics and climate, this work shows that these effects are more complex than currently thought.

1. Introduction

Black Carbon (BC) has important effects on climate, owing to its ability to absorb incoming shortwave radiation. Heating of airmasses containing BC are predicted to lead to changes in large-scale atmospheric circulation [*Hansen et al.*, 1997]. On smaller scales, heated airmasses can also exhibit increased static stability, reducing convective activity and cloud coverage [*Ackerman et al.*, 2000]. *Lohmann and Feichter* [2001] studied the competition between BC warming and sulfate indirect aerosol cooling and concluded that sulfate cooling prevails globally. The authors note that their simulations likely underestimate BC effects, since they neglected the enhancement of BC absorption when included within cloud droplets [*Chýlek et al.*, 1996; *Fuller et al.*, 1999].

Heat released by BC included within the CCN populations can also hinder their ability to activate; the energy absorbed acts to increase the droplet temperature and the critical supersaturation [*Conant et al.*, 2002, hereafter referred to as "Part 1"]. The change in cloud condensation nucleus (CCN) activation spectrum from this heating was studied in Part 1; a reduction in CCN concentration between 1 and 10% (depending on the cloud parcel maximum supersaturation and the CCN BC mass fraction) is seen when compared to the same CCN without heating present.

For typical atmospheric conditions, the reduction in CCN from BC heating is expected to be on the order of a few percent. Although these changes are minor, numerous microphysical (and previously unaccounted)

mechanisms arise that can magnify the effect on the droplet population. One of the reasons for this is that BC heating selectively affects CCN with a low critical supersaturation, S_c. Although these particles would eventually form droplets in typical cloud updrafts, their transformation is delayed compared to the rest of the CCN population; this delay allows water vapor, which would otherwise condense on these larger CCN, to condense on aerosol of higher S_c. Second, the energy released from the radiative heating will conduct into the gas phase, affecting parcel temperature and supersaturation. Finally, additional dynamical adjustments in the cloud supersaturation (because of the change in droplet number and cooling rate) can further change the supersaturation profile that develops in the cloud. Depending on the dominant mechanism, BC heating can either decrease or increase the droplet concentration throughout the cloud column.

Droplet number concentration can also be affected by another mechanism previously unaccounted for: by decreasing the efficiency of Giant Cloud Condensation Nuclei (GCCN, here defined as particles that have a diameter larger than 5 μm) in initiating the formation of drizzle. It is well known that GCCN can form haze drops that are large enough to initiate drizzle formation. Usually, the size needed to be attained to initiate drizzle is about 38-40 μm diameter [*Feingold et al.*, 1999]. When BC is present in these particles, their growth can be slowed down enough to decrease their size and ability to form drizzle. If this happens, the cloud droplet number concentration would increase (when compared to a non-heated cloud, where drizzle has formed), potentially leading to a more reflective and persistent cloud.

If all these aerosol-cloud interactions are important, then knowledge of the total BC heating rate (an approach used in previous studies) is not sufficient to fully characterize BC effects on climate; additional information regarding the size distribution and mixing state of BC (within the CCN population) and the influence on cloud droplet concentration is necessary.

We estimate here the potential climatic significance of the BC-cloud microphysical mechanisms previously identified. A cloud parcel model with explicit microphysics, modified to account for the effects of radiative absorption on the gas-phase and droplet energy balance, is used to simulate the growth of CCN to form cloud droplets. Simulations are carried out for a suite of conditions representative of regions with varying degrees of anthropogenic influence and aerosol mixing state so that the importance of each mechanism (including those that tend to increase cloud drop number and albedo) is explored. In assessing the effect of radiative heating on the ability of giant CCN to initiate precipitation we also use a parcel model coupled with Lagrangian trajectories derived from an LES simulation of a stratocumulus cloud.

2. Effects of BC heating on cloud microphysics

Here we discuss in depth the various mechanisms that were briefly touched upon in the introduction. Since all the mechanisms studied in this work result from BC warming, the term "positive feedback", is used to characterize a mechanism that tends to further warm the climate system (usually because of a decrease in cloud droplet number), while "negative feedback" is used for characterizing cooling mechanisms (usually because of an increase in cloud droplet number).

2.1. Extended Köhler theory

It has been shown (Part 1) that in addition to providing insoluble material, BC can heat up a droplet sufficiently to change its CCN activation characteristics. This effect can be expressed in terms of a modified Köhler equation for the equilibrium saturation ratio, S_{eq},

$$S_{eq} = \exp\left[\frac{A\,(1+\gamma_a)}{D_p} - \frac{B}{D_p^3 - d_u^3}\right] \qquad (1)$$

$\gamma_a = \frac{\rho_w \Delta H_v \Phi}{8\sigma\pi k_a' T}$ is the so-called "heating parameter", where ΔH_v latent heat of condensation of water, Φ is the heating rate per particle, ρ_w density of water, σ water surface tension, T is the droplet temperature and k_a' is the thermal conductivity of air. Furthermore, D_p is the wet diameter, d_u is the diameter of the insoluble core, and $A = \frac{4M_w\sigma}{RT\rho_w}$, $B = \frac{6n_s M_w}{\pi\rho_w}$, are standard Köhler theory parameters, with M_w being the molecular weight of water, R is the universal gas constant, and n_s is the number of moles of ions in solution. Φ is sensitive to the radiation field, the mass of black carbon in the droplet, and the diameter of the droplet. Generally Φ increases with increased BC mass, although the rate of increase is a complex function of the size and geometry of the BC inclusion and the droplet. Part 1 provides a detailed discussion of this dependence for the simple case of a spherical BC inclusion at the center of the droplet under cloud-free skies. The uncertainty in Φ associated with these simplifications is generally within 50%.

Radiative heating changes the Köhler curve by multiplying the Kelvin term A/D_p with a factor of $(1+\gamma_a)$.

This tends to increase the critical supersaturation, S_c, of CCN (because $\gamma_a > 0$) and implies that fewer CCN will tend to activate (under constant ambient supersaturation) than in the absence of heating. Thus, this effect represents a positive feedback since the decreased droplet concentration would lead to less reflective clouds and diminish their cooling effect. This implicitly assumes that supersaturation and liquid water profiles within a cloud do not change, whether radiative heating is present or not. Dynamical adjustments and gas-phase heating can change parcel supersaturation profiles between heated and non-heated CCN; these effects have to be considered for a comprehensive assessment of BC on droplet number.

2.2. Dynamical adjustments in cloud supersaturation

Dynamical adjustments are seen in cloud supersaturation whenever the CCN population changes. In the case of BC heating, the lower critical supersaturation portion of the "CCN spectrum" (defined as the number of CCN that can activate as a function of supersaturation) shifts towards higher S_c; this physically means that the rate of water absorption in the early stages of cloud formation is decreased (since fewer particles activate). As a result, the parcel S_{max} increases accordingly, until enough droplets form to consume the available water vapor. This response in parcel supersaturation acts to restore the original cloud droplet number.

Dynamical adjustments in parcel supersaturation can lead to non-monotonic activation behavior. For example, when seasalt and sulfate compete as CCN, under certain conditions the presence of additional CCN can lead to a decrease (as opposed to an increase) in droplet number [*Ghan et al.*, 1998; *Smith et al.*, 1996]. In the case of radiative heating, the opposite may happen: by selectively inhibiting low S_c particles from scavenging water vapor (which has been shown in Part 1 to be the main effect of BC heating on droplet thermodynamics), particles of higher S_c, which are less susceptible to kinetic limitations [*Nenes et al.*, 2001] and more numerous, may compensate for the initial loss in droplets.

2.3. Gas-phase heating

Heat released from the particles to the gas phase has an influence on parcel supersaturation, because the effective parcel cooling rate is decreased. This tends to decrease the cloud maximum supersaturation, S_{max}, and fewer CCN will tend to activate. The result is lower droplet concentrations and liquid water, and with it, decreased cloud optical depth and albedo. This means that gas-phase heating can have a positive climate feedback, i.e. additional warming, from decreased cloud coverage and albedo. This type of feedback is different from the "semi-direct" mechanism proposed by *Hansen et al.* [1997], because it reflects the effect of gas-phase warming on parcel supersaturation and cloud droplet number, not on static stability and the consequences thereof.

It should be noted that the previous discussion assumes the CCN spectrum between heated and non-heated parcels remain the same. This is not true if the BC is contained within the CCN; in this case, the nonlinear interplay between droplet number, cloud supersaturation and liquid water need to be considered. The knowledge of ambient meteorological conditions and CCN spectrum may not be sufficient to fully describe droplet formation. It is possible that two identical CCN spectra, one corresponding to pure salt and one composed of a mixture of salt and BC, still produce different droplet concentrations for identical meteorology (because gas-phase heating in the second population lowers the S_{max} compared to the first aerosol). This is an important point; traditional thinking holds that identical CCN spectra yield the same droplet concentrations for given ambient conditions.

Gas-phase heating effects can be important even for negligible changes in the CCN spectrum. Cases where this will happen are if: *i*) the absorptive species are located primarily in the smaller CCN (so that γ_a for each droplet becomes negligible), *ii*) absorptive species are externally mixed in the CCN population, or, *iii*) the parcel S_{max} is outside the region of influence of radiative absorption on the CCN (i.e. is not on the "lower end" of the spectrum), but the BC heating rate is comparable to the parcel cooling rate.

Heating of the gas phase can be important without appreciable changes in the CCN spectrum, but the reverse is not seen; important gas-phase heating is always present when the number of CCN are influenced by BC inclusions. This can be illustrated by the following order of magnitude calculation. It was shown in Part 1 that a heating parameter $\gamma_a \approx 0.1$, or a heating rate of order 10^{-9} W per particle, is required for a droplet to experience appreciable changes in its S_c. Assuming $\gamma_a = 0.1$ and that radiative heating affects 10 drops cm^{-3} (which is a few percent of the total droplet concentration for polluted conditions) and that BC is contained only in these 10 drops, a total heating rate of 10^{-5} K s^{-1} is computed (assuming $c_{p,air} = 10^3$ J kg^{-1} K^{-1}, and $\rho_{air} = 1$ kg m^{-3}). An updraft of 10^{-2} m s^{-1}, following a moist adiabat of

-5.8×10^{-3} K m^{-1} (which corresponds to 1000 mbar and 273 K), produces a cooling rate of -5.8×10^{-5}K s^{-1}. We observe that the BC heating rate and the updraft cooling rates are of the same order, meaning that the parcel (in this example) experiences a non-trivial decrease in cooling rate. As a result, parcel supersaturation, being a strong function of cooling rate, will also drop. Thus, even for conditions where gas-phase heating is minimum and droplet number is maximum, gas-phase heating cannot be neglected. In reality, particles containing BC can reside in the interstitial aerosol, further increasing the heating rate.

An important issue is the resulting effect of gas-phase heating on the cloud dynamics. An immediate effect of the released heat is to increase the buoyancy of the cloud parcel; this would tend to accelerate the cloud parcel, and effectively lead to additional activation of cloud droplets. The former effect is another negative feedback, since the additional activated CCN can enhance cloud albedo. This is an effect relevant for activation timescales ($\sim$ 1 min), as for longer timescales, radiative heating tends to destabilize the stratocumulus cloud layer by decreasing the efficiency of radiative cooling at the top of the cloud layer [*Ackerman et al.*, 2000; *Ackermann and Toon*, 1996]. All these effects can be adequately addressed only with a full cloud resolving model, so, for the purposes of this study, we decouple the feedback of BC heating on parcel dynamics with the intent of addressing these issues in the future.

2.4. Effect of aerosol mixing state and composition on heating effects

A consequence of the gas phase-droplet energy coupling is that the mixing state of the BC within the CCN population may play an important role in the overall effects of BC heating on cloud microphysics. This is embodied in the following question: "If the BC is assumed to heat only the gas phase, without perturbing the CCN spectrum (i.e. an externally mixed BC population), how would the resulting cloud compare, in terms of droplet number and aerosol optical properties, to that when the BC is internally mixed in the CCN population?" In lieu of the feedback mechanisms, it becomes unclear which mixing state would produce fewer drops and liquid water content (LWC).

2.5. Effect of heating on GCCN

While black carbon is normally associated with particles of submicron size, an interesting, and unrecognized, effect of BC absorption on the growth of GCCN arises if absorbing material is present in such particles: by changing the behavior of giant CCN (GCCN), defined as particles with a dry diameter larger than 5 μm. Numerous studies (e.g., *Feingold et al.* [1999]) have investigated the catalytic role of GCCN in initiating precipitation. For situations in which absorbing material is present in large enough quantities, radiative heating can delay their growth; if this happens, the number of collector drops will decrease, and the probability for drizzle formation is reduced. In contrast to the radiative heating effects on the gas phase and CCN spectrum, the effect on giant CCN constitutes a (counter-intuitive) negative climate feedback, i.e. this mechanism of BC heating would tend to *increase* the lifetime of clouds, and thus enhance their cooling effect.

3. Effects of BC heating on cloud droplet number

3.1. Cloud parcel and albedo models

To address all of the heating effects quantitatively, we simulate cloud albedo and droplet number concentration using an adiabatic cloud parcel model with explicit aerosol microphysics. The model of *Nenes et al.* [2001] is used, with two modifications. First, Equation (1) is used for computing S_{eq} in the droplet growth rates, and second, the energy released by BC absorption is included in the gas-phase (parcel) energy balance. γ_a is computed online, from the BC content and droplet diameter.

Cloud albedo, R_c, is estimated based on the two-stream approximation of a non-absorbing, horizontally homogeneous cloud [*Lacis and Hansen*, 1974],

$$R_c = \frac{\tau}{\tau + 7.7} \tag{2}$$

where τ is the optical depth, computed from the liquid water and effective radius profiles in the cloud. The effective radius is computed as the ratio of the third over the second moment of the droplet size distribution. Equation (2) neglects the reduction in single-scattering albedo from the presence of BC in the cloud, so that albedo changes are only a result of changes in effective radius and liquid water content.

The optical depth and albedo calculations we present here are not intended to be used for prognostic purposes, but only to diagnose the sensitivity of droplet nucleation and condensational growth to changes in the CCN population from the radiative heating. For this purpose, the use of Equation (2) should suffice. Expressing changes in terms of changes in effective radius

and albedo gives a physically-based measure of the importance of heating effects. This is important because albedo is sensitive not only to droplet concentrations, but also to changes in the LWC (which is important when the gas phase is heated). An analysis using effective radii and droplet concentrations cannot capture this dimension.

3.2. Aerosol distributions and simulation scenarios considered

It was shown in Part 1 that the CCN spectrum for pristine conditions is not significantly affected by heating; therefore, we focus primarily on aerosol representative of polluted airmasses. The urban aerosol size distribution of *Whitby* [1978] is used (Table 1), with an aerosol assumed to be composed of BC (or insoluble material) and $(NH_4)_2SO_4$. Updraft velocities of 0.10, 0.25 and 0.50 m s^{-1} are examined. An emphasis is given to low values, since the BC heating effects are most prominent at low updraft (or cooling) rates. The initial parcel temperature, pressure and relative humidity are 298K, 800 mbar, and 96% respectively. BC warming is assumed to begin from cloud base, i.e. the parcel does not experience heating until it reaches saturation. In reality, the parcel containing BC will experience heating even before it becomes saturated, and thus, will differ from the non-heated parcel. We chose to neglect this in order to have consistent LWC fields, and initial aerosol sizes at cloud base. We do not consider the vertical variation of actinic flux with cloud height. The heating rates Φ are computed using the procedure presented in Part 1.

Four heating "scenarios" are considered in the parcel simulations. The first is a simulation in the absence of radiative heating altogether ("NoHeat" scenario). In this case, the black carbon core acts solely as an insoluble inclusion. The second scenario assumes radiative heating to be present, but allows only for changes in the droplet thermodynamics ("Drop" scenario); that is, the droplet attains the steady state temperature profile and heats up, but no conduction of energy occurs into the gas phase. This scenario extends the analysis of Part 1 to find the effect of BC droplet heating on cloud activation. The third scenario represents a situation in which BC radiative heating influences only the gas phase. This scenario, referred to as "External", corresponds physically to a CCN population that contains a non-BC insoluble core externally mixed with a BC population that produces a total heating rate equal to that of the "Drop" scenario. Finally, a fourth scenario, named "Internal", represents the opposite situation where the black carbon is contained within the CCN, and the heat generated from the radiative absorption is allowed to affect both the gas-phase energy balance and the droplet thermodynamics. The four scenarios are illustrated in Figure 1.

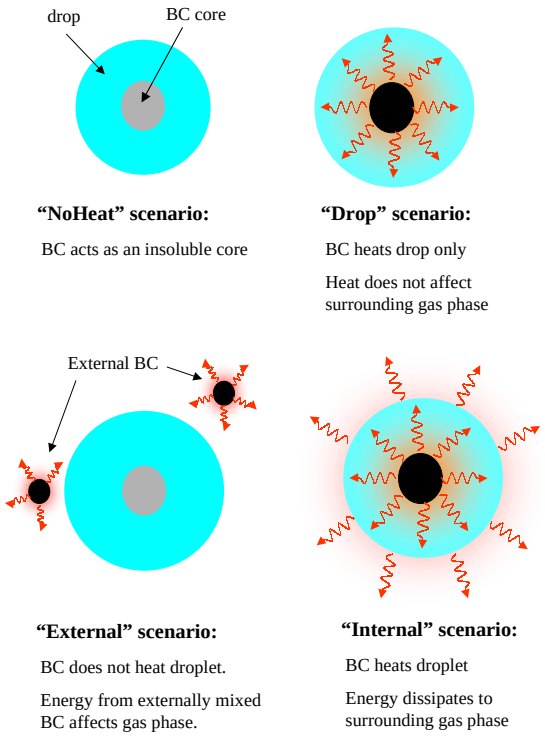

Figure 1. Illustration of the BC heating scenarios considered in this study.

Evaluating these four scenarios gives a comprehensive picture of the effect of radiative heating on droplet formation. The total heating rate, when BC is present, is the same among the scenarios, and the critical supersaturation spectra of the aerosol, in the absence of radiative heating, are identical. Thus, differences in cloud droplet number and cloud properties among the scenarios are due solely to the location of the heating and the feedbacks allowed to exist.

4. Dynamical simulations

Aerosol heating effects are quantified by comparing cloud albedo and effective radius between any two heating scenarios. The resulting difference, ΔR_c, in cloud

Table 1. Aerosol distribution parameters (geometric radius $r_{g,i}$ in μm, number concentration N_i in cm^{-3}) [*Whitby*, 1978]

Aerosol type	Nuclei Mode			Accumulation Mode			Coarse Mode		
	$r_{g,1}$	σ_1	N_1	$r_{g,2}$	σ_2	N_2	$r_{g,3}$	σ_3	N_3
Marine	0.005	1.6	340	0.035	2.0	60	0.31	2.7	3.1
Urban	0.007	1.8	106000	0.027	2.16	32000	0.43	2.21	5.4

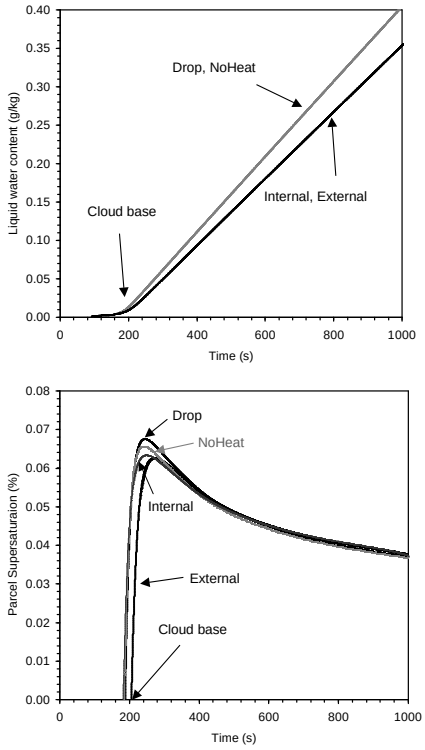

Figure 2. Parcel liquid water content (a) and supersaturation (b) profiles for four different radiative heating scenarios. Updraft velocity is 0.25 m s^{-1} and BC content is 50%.

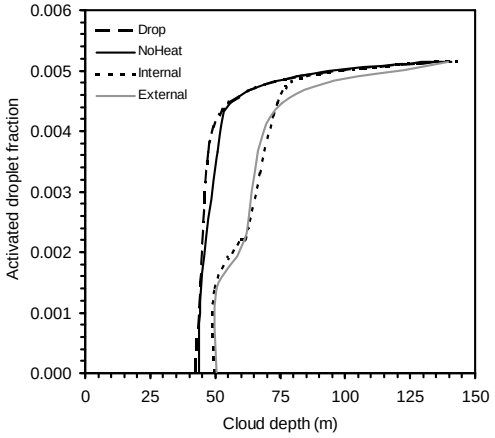

Figure 3. Parcel droplet activation ratio for the simulations of Figure 2.

albedo for a cloud of the same depth is a direct measure of the change exerted on the optical properties of a cloud.

Figures 2, 3 present typical parcel supersaturation, liquid water content and cloud droplet profiles for the different heating scenarios. The updraft velocity in these simulations is 0.25 m s^{-1}, while the aerosol is assumed to be 50% BC (the large value of BC fraction was selected so that the effects of heating on the parcel LWC and supersaturation are clearly identified). As expected, the liquid water contents of the "NoHeat" and "Drop" scenarios are the same (after cloud base is reached). This is because the in-cloud lapse rates are identical, as a result of the gas-phase energy balance being identical in these two cases. Similarly, the liquid water content profiles of the "External" and "Internal" scenarios are similar, but differ from the "NoHeat" scenario. The cloud maximum supersaturation varies by 10% for the different heating scenarios when compared to the "NoHeat" scenario (S_{max} = 0.0660%); supersaturation increases in the "Drop" scenario (S_{max}= 0.0695%), and decreases for the "External" (S_{max}= 0.0630%) and "Internal" (S_{max}= 0.065%) scenarios. These supersaturations are within the range of reported values for polluted stratocumulus clouds and fogs [*Hop-*

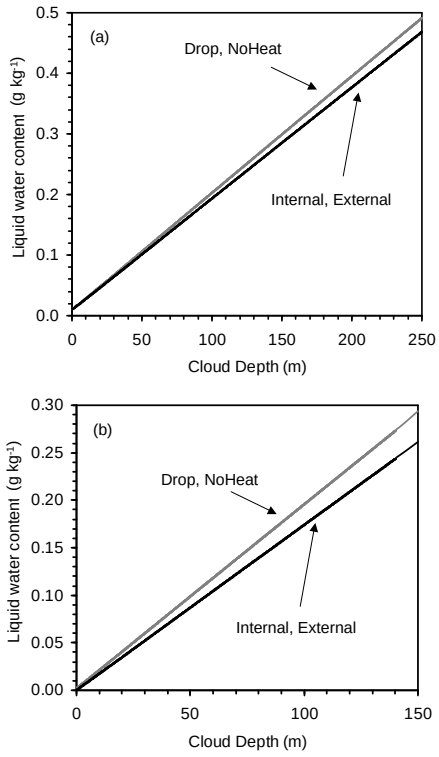

Figure 4. Liquid water content between heating scenarios as a function of cloud depth. The BC mass fraction is (a) 0.1, and (b) 0.2. The updraft velocity is assumed to be 0.1 m s^{-1}.

pel et al., 1996; *Hudson*, 1983]. The changes in S_{max} may appear small, but are sufficient to reflect important changes in particle growth kinetics between the scenarios (Figure 3); the "Drop" scenario responds the quickest to form droplets, due to the accelerated response of higher S_c CCN. The "NoHeat" scenario responds almost as fast, while the "Internal" and "External" scenarios take longer to form droplets. The "Internal" scenario, for the same reasons as "Drop" forms droplets more quickly than "External", which even at 125 m cloud depth has not formed all of its droplets. The S_{max} values for these simulations correlate well with the droplet activation behavior shown in Figure 3.

We now examine lower BC fractions, which are within atmospheric observations. Figures 4 and 5, shows the liquid water content, and the albedo difference between heating scenarios, as a function of cloud depth. The BC mass fraction is 0.1 and 0.2, and the updraft velocity is assumed to be 0.1 m s^{-1} The presence of radiative heating has an important effect on cloud properties. This can be seen in the values of effective radius and S_{max} (Table 2). The "Drop" effective radius is slightly smaller than for "NoHeat" in the initial stages of the cloud; dynamic adjustment mechanism in cloud supersaturation, which tends to form slightly more droplets in the "Drop" scenario. As a result, the "Drop" scenario leads to slightly higher optical depths and albedo. The situation is quite different for the "External" scenario, where differences in albedo with "NoHeat" can be explained from the reduced parcel LWC in the former scenario (even though the effective radius is smaller than in the "NoHeat" scenario). The maximum albedo difference between the two scenarios is 0.009 for 10% BC and 0.024 for 10% BC, at a cloud depth of 150 m. The albedo difference for the "Internal" and "External" scenarios look similar. The "Internal" scenario however exhibits the smallest albedo difference; given their identical LWC, the difference arises from changes in effective radius (which is a result of the different timescales of droplet formation). S_{max} varies between 4 and 5%, while effective radius varies between 2 and 4 %.

Simulations for other updrafts indicate that, whenever the heating rate is non-negligible (compared to the adiabatic cooling rate), an effect is seen on cloud properties. The magnitudes of each feedback of course vary, but both positive and negative feedbacks are seen. What also can be seen in the Figure 5 is that the mixing state of the black carbon can have an important effect on the cloud optical properties. As the LWC between the "Internal" and "External" scenarios are the same, this difference is due to the dynamical readjustments in parcel supersaturation. Furthermore, the simulations indicate that the assumption of externally mixed BC with the CCN population would tend to maximize the effects of BC heating. We should note that we have assumed the same gas-phase heating rate from the BC, regardless of its mixing state within the CCN population. In reality, externally mixed BC would heat the parcel less efficiently [*Chýlek et al.*, 1996; *Fuller et al.*, 1999]; the difference between mixing states may therefore be smaller, but qualitatively unchanged.

5. Radiative heating and Giant CCN

It can be shown that, based on its effect on critical supersaturations, BC does not increase the S_c of GCCN enough to inhibit their strict activation for supersaturation typically found in clouds. However, the

Table 2. Effective radius (at 140 m cloud depth) and maximum supersaturation (%) for the parcel simulations in Figures 4 and 5.

Simulation	r_{eff}, 10% BC	r_{eff}, 20% BC	S_{max}, 10% BC	S_{max}, 20% BC
External	5.17	5.20	3.00×10^{-2}	3.12×10^{-2}
Internal	5.15	5.26	3.05×10^{-2}	3.17×10^{-2}
Drop	5.21	5.33	3.12×10^{-2}	3.35×10^{-2}
NoHeat	5.24	5.36	3.08×10^{-2}	3.27×10^{-2}

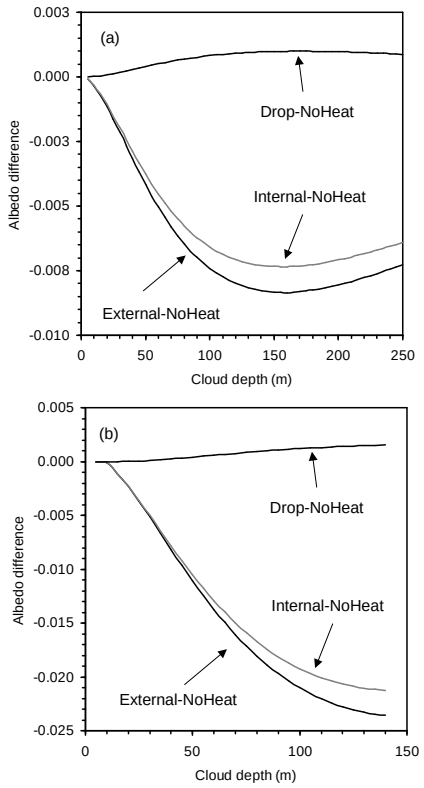

Figure 5. Albedo difference between the curves of Figure 4, as a function of cloud depth.

critical radius of GCCN is too large (hundreds of μm or larger) to be attained in clouds through the mechanism of diffusional growth, and GCCN can effectively initiate precipitation at much smaller sizes that its critical diameter. Therefore, it is necessary to study the kinetics of GCCN growth in order to get a more comprehensive picture of the sizes these particles attain in clouds.

Two approaches are used in order to study the growth of GCCN. In the first approach, we use simple adiabatic cloud parcel theory to assess the time needed for GCCN to grow to a large enough size to effectively initiate drizzle formation. This approach allows us to systematically explore parametric space and determine the conditions of updraft velocity and particle size for which BC heating effects are expected to become important. The simulations are carried on by exposing a BC-containing particle to supersaturation profiles computed with the adiabatic cloud parcel model. The lognormal distributions by *Whitby* [1978], which are used in our simulations, include nucleation, accumulation, and coarse modes. The presence of a coarse mode ensures that we include the effect of GCCN on parcel supersaturation, which can be important [*Ghan et al.*, 1998]. BC is included only in one particle, while the rest of the CCN are assumed to be composed of $(NH_4)_2SO_4$. The BC-containing particle is initially assumed to be dry and then allowed to grow as the supersaturation profile develops; the GCCN is assumed to follow the parcel without dropping out. The portion of cloud for which these GCCN are smaller than the threshold size of 40 μm diameter (larger particles have a high collection efficiency and for ambient concentrations can initiate precipitation) are examined with and without radiative heating. Collision and coalescence processes are not considered in these simulations. Furthermore, we assume that ventilation effects are not important, so that the transfer of heat from the droplet to the gas phase is primarily from conduction. This assumption

holds reasonably well up to 50 μm in diameter [*Smolik et al.*, 2002].

Although useful, the adiabatic parcel simulations reflect idealized cloud parcels. A second approach is therefore necessary, to verify that the insight obtained from simple parcel theory can also be applied to a more realistic description of GCCN growth in clouds. This is realized by adopting the Trajectory Ensemble Model (TEM) of *Stevens et al.* [1966], in which a set of 500 trajectories derived from a Large Eddy Simulation (LES) of a non-precipitating marine stratocumulus deck is used to "drive" a non-adiabatic parcel model and compute supersaturation profiles. GCCN are exposed to the supersaturation profiles (using the same procedure as in the adiabatic parcel profile simulations) and are allowed to grow with and without radiative heating present. Horizontal and temporal (one-hour) ensemble averages are then computed for the GCCN size throughout the cloud column. The portion of cloud for which GCCN are smaller than the threshold size (40 μm wet diameter) is examined with and without radiative heating.

A typical stratocumulus cloud was selected for the TEM. This cloud an average liquid water content of about 0.3 g kg^{-1}, while the average vertical velocity (updrafts and downdrafts), average and maximum updraft velocity of the stratocumulus cloud are shown in Figure 6, as a function of height. This cloud selected is both well developed and energetic enough to ensure that the GCCN will remain in the cloud. Two types of CCN are used to compute the supersaturation trajectories: one representing pristine (marine size distribution of *Whitby* [1978]) and one representing polluted conditions (urban size distribution of *Whitby* [1978]). The aerosol is assumed to be composed of $(NH_4)_2SO_4$.

Figure 7 shows the growth of GCCN throughout an adiabatic cloud column that experiences an updraft of 0.25 m s^{-1} (the "NoHeat" scenario of the previous section is used to generate the supersaturation profile). The composition of the BC-containing GCCN is assumed to be 10% $(NH_4)_2SO_4$, 0-20% BC, the remaining mass being insoluble material. The rest of the CCN are composed of pure $(NH_4)_2SO_4$. The particle dry diameter is allowed to vary between 5 and 10 μm. GCCN that contain BC are assumed to experience radiative heating, so that a particle with 0% BC has the same amount of insoluble material as one with 10% BC, but experiences no heating. By examination of the growth curves we can see that the GCCN that contain BC and have a dry size of 5 μm practically never grow beyond 40 μm in size; without BC, the same particles would easily exceed 40 μm. As expected, a larger BC content

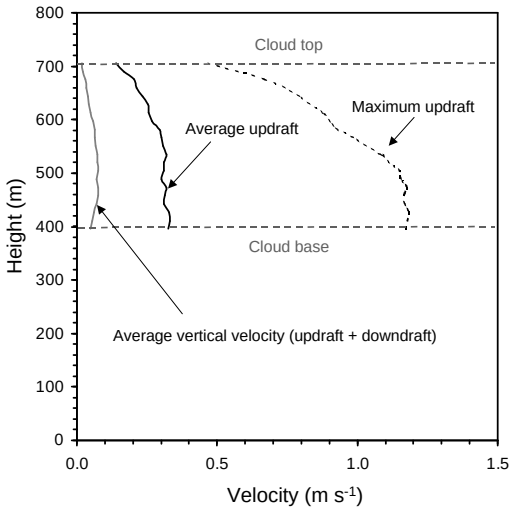

Figure 6. Vertical profiles of average vertical velocity (updrafts and downdrafts), average and maximum updraft velocity for the stratocumulus cloud trajectories used in this study.

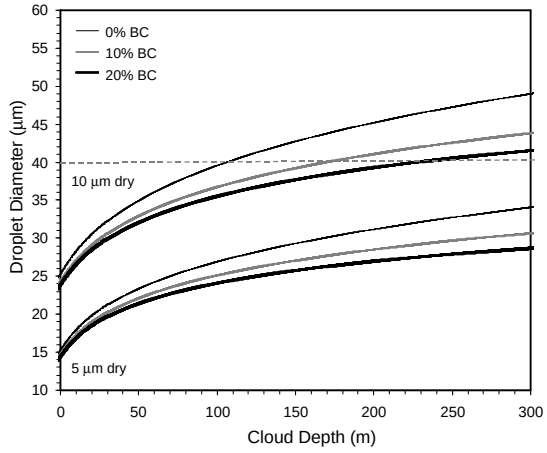

Figure 7. Growth of GCCN throughout a cloud column that experiences an updraft of 0.25 m s^{-1} (the "NoHeat" scenario of the previous section is used to generate the supersaturation profile). The composition of these particles is assumed to be 10% $(NH_4)_2SO_4$, 0-20% BC (the rest is dust). Curves are shown for particles with dry diameter of 5 and 10 μm. The dashed line represents the threshold size above which the collection efficiency of the droplets is assumed to become large.

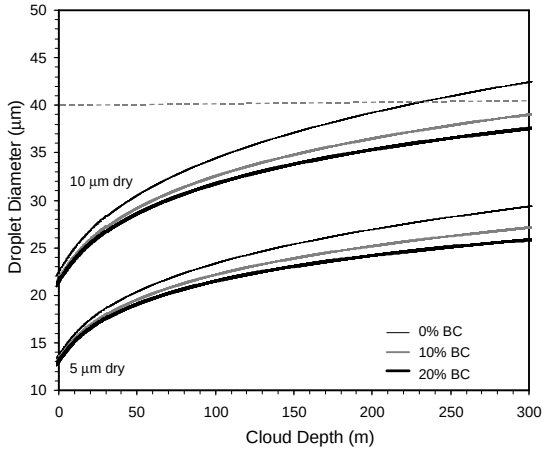

Figure 8. Same as Figure 7, but for an updraft velocity of 0.5 m s^{-1}.

tends to decrease the growth rate of the droplet. Therefore, particles of 5 μm dry diameter containing BC are effectively inhibited from reaching a size that is generally considered necessary for initiating precipitation. Even for particles that have a dry diameter of 10 μm, the presence of BC can substantially reduce their ultimate size (43-46 μm with BC vs. 50 μm without BC), although still large enough to act as collector drops.

The behavior seen in Figure 7 is also seen for larger updraft velocities. Figure 8 shows the growth of GCCN throughout a cloud column that experiences an updraft of 0.5 m s^{-1} (the "NoHeat" scenario of the previous section is used to generate the supersaturation profile), with the same GCCN as in Figure 7. Compared to Figure 7, particles grow to smaller sizes. This is because in stronger updrafts, droplets have less time for condensational growth. Therefore, the presence of BC is even more effective in prohibiting drizzle formation, since less BC per particle is necessary to keep the droplet below the threshold size. Given these results, one would expect to see that a further increase in updraft velocity would render GCCN even more susceptible to BC inclusions. Indeed, simulations performed for updrafts

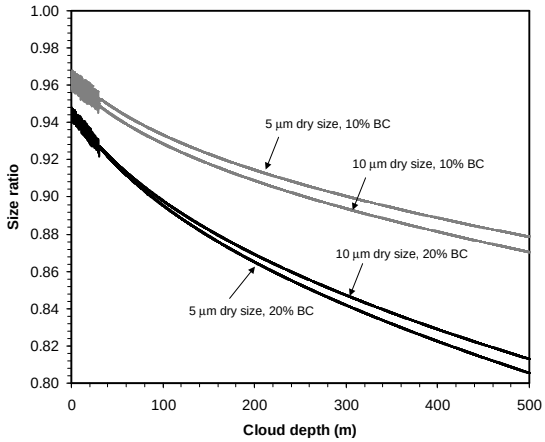

Figure 9. Normalized droplet sizes of the heated GCCN with respect to their unheated size, for the curves in Figure 7

velocities of 0.5 and 1.0 m s^{-1} (not shown) confirm this.

An interesting feature of the GCCN growth curves is illustrated in Figure 9, which shows the normalized droplet sizes of the heated GCCN with respect to their unheated size, for the curves in Figure 8. The figure suggests that the size difference between a heated and non-heated GCCN increases as the particle traverses the cloud column. This is an important feature; this means that heated drops will *always* be smaller than unheated drops, and that this size difference will become *larger*

with time. As the updraft velocity increases, the normalized ratio decreases, which means that the size difference becomes larger. Another striking feature is that the normalized droplet size curves of the same BC content seem to collapse onto each other. This implies that particles, regardless of their dry size (and critical supersaturation), experience approximately the same (relative) decrease in their size.

One might suspect that the behavior illustrated in Figure 9 is a consequence of the supersaturation profile (and hence the driving force for particle growth) that decreases as the cloud drops rise further up in the cloud column. This is not true. We will demonstrate this behavior is not unique to adiabatic parcels with smooth supersaturation profiles, but can be expected for any randomly-fluctuating positive supersaturation environment (such as that existing in real clouds). Starting from Equation 1, we can relate the equilibrium saturation ratio of a GCCN that experiences radiative heating, S^w_{eq}, to the equilibrium saturation ratio of a GCCN that does not experience radiative heating, S^{wo}_{eq}:

$$S^w_{eq} = S^{wo}_{eq} + \frac{A\gamma_a}{D_p} \tag{3}$$

The rate of growth for the GCCN particle with radiative heating is [*Nenes et al.*, 2001] :

$$\frac{dD^2_{p,w}}{dt} = 2G(S - S^w_{eq}) \tag{4}$$

where G is a function of T,P and S is the parcel saturation ratio. Substituting Equation 3 into 4, and given that the rate of growth of the GCCN in the absence of radiative heating, $\frac{dD^2_{p,wo}}{dt} = 2G(S - S^{wo}_{eq})$, we obtain:

$$\frac{dD^2_{p,w}}{dt} = \frac{dD^2_{p,wo}}{dt} - \frac{2GA\gamma_a}{D_{p,w}} \tag{5}$$

Assuming that $(D_{p,w}+D_{p,wo}) \approx 2D_{p,w}$ and defining the quantity $\Delta D_p = D_{p,w} - D_{p,wo}$, Equation 5 becomes:

$$\frac{d\Delta D_p}{dt} = -\left(\frac{2GA\gamma_a + 2Gs\Delta D_p}{D^2_{p,w}}\right) \tag{6}$$

where s is the parcel supersaturation, $S - 1$. Given that $S^w_{eq} \approx 1$, then $S - S^w_{eq} \approx s$, and Equation 4 can be integrated over the supersaturation history to give the GCCN diameter at any time:

$$D^2_p = d^2_p + 2G\int_0^t s(\tau)d\tau \tag{7}$$

where d_p is the dry diameter of the GCCN (we assume the particle to be dry at t=0). Substituting Equation 7 into 6 gives:

$$\frac{d\Delta D_p}{dt} = -\left(\frac{A\gamma_a + s\Delta D_p}{\frac{d^2_p}{2G} + \int_0^t s(\tau)d\tau}\right) \tag{8}$$

Equation 8 expresses the rate of change of ΔD_p (which is the difference in size of a GCCN for when it experiences radiative heating and when it does not, for identical supersaturation history), as a function of the supersaturation history, γ_a and the dry diameter. Under the condition of a supersaturated environment, the right hand side of the equation is always negative. This means that a GCCN that experiences heating will always be smaller than if it were not heated. Furthermore, the magnitude of ΔD_p will grow continuously with time, with a rate that depends on the specific cloud supersaturation history. Equation 8 also explains the weak dependence of the size ratio in Figure 9 on the GCCN dry diameter: for small exposure times, the absolute value of ΔD_p is small, while for long exposure times, $\frac{d^2_p}{2G} \ll \int_0^t s(\tau)d\tau$, and so the denominator of the right hand side will lose its dependence on d_p. Equation 8 also shows that γ_a (or % BC content) has a strong influence on the magnitude of ΔD_p, which is also seen in Figure 9.

The TEM simulations confirm what was seen in the adiabatic parcel calculations, despite the substantial differences between the two cloud models. Figure 10 shows the average size of 5 μm (dry diameter) GCCN as predicted by the TEM for (a) pristine cloud conditions and (b) polluted cloud conditions. The black dashed line indicates cloud base, while the grey dashed line indicates the size beyond which a GCCN can effectively initiate drizzle formation. One can observe the characteristic increase of the GCCN size for increasing cloud depth, indicative of the larger residence times experienced by parcels that reach deep into the cloud. The effect of radiative heating is significant: in the presence of BC, the size of the GCCN is always smaller than 40 μm. Particularly interesting is that without the presence of radiative heating, GCCN will exceed the threshold of 40 μm for the pristine cloud; this does not happen once BC is present in the particles. Another interesting feature is that throughout the cloud column, the size ratios of GCCN with 10% BC to those with 0% BC is around 0.9, and the size ratio for particles with 20% to those with 0% BC is around 0.85. The fact that these ratios remain almost constant throughout the cloud can be explained from Equation 8: given that the supersat-

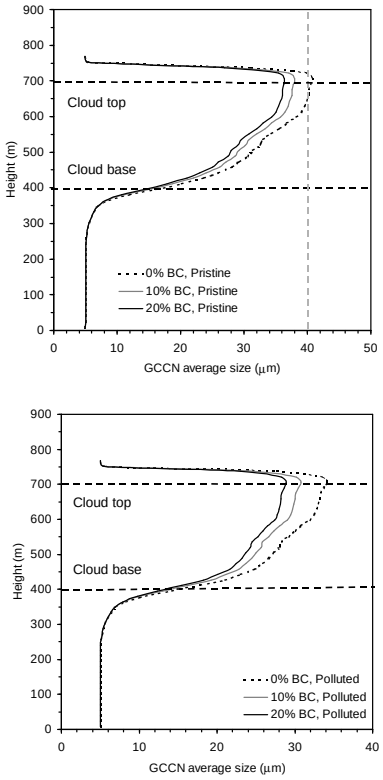

Figure 10. Average size of GCCN as predicted by TEM for (a) pristine cloud conditions and (b) polluted cloud conditions. The dry diameter of the GCCN is assumed to be 5 μm. The black dashed line indicates cloud base, while the grey dashed line indicates the size beyond which the GCCN is assumed to effectively initiate drizzle formation.

uration profiles do not change between curves (because the same trajectories are used for GCCN of different BC content), the ΔD_p will depend primarily on BC content.

When larger GCCN are used in the trajectories, similar behavior to Figure 10 is obtained. This is illustrated in Figure 11, which is same as Figure 10, but for a GCCN dry diameter of 10 μm. The effect of radiative heating is significant, although the decrease in size is insufficient in pristine clouds to make the GCCN smaller than 40 μm. Another interesting feature is that throughout the cloud column, the size ratios of GCCN with 10% BC to 0% BC is between 0.88-0.9, and the size ratio for particles with 20% to 0% BC is around 0.85. The stability of the size ratios throughout the cloud can be explained, just like before, from Equation 8. What is surprising is that the size ratios remain relatively constant between the pristine and polluted clouds. Furthermore, the size ratios are consistent with those ratios obtained from adiabatic parcel theory for a 0.25 m s^{-1} updraft (Figure 9), which is the average vertical velocity for the updrafts (Figure 6). This suggests that perhaps BC content primarily controls the size reduction of GCCN from BC heating, and to a lesser degree, supersaturation history statistics.

6. CONCLUSIONS

The effect of radiative heating on cloud droplet number concentration and cloud optical properties can be important for conditions characteristic of polluted, aged aerosol with a significant fraction of black carbon (BC). The sign of the climatic feedback from BC effects on cloud microphysics can be either positive or negative, rendering the overall BC influence on climate even more complex than previously thought. Two effects of BC radiative heating can increase cloud droplet concentration: *i*) the effect of BC on the ability to decrease the collection efficiency of giant CCN, and, *ii*) the delayed growth of low S_c CCN that permits CCN of higher S_c to form drops. These two mechanisms complement each other in terms of increasing the cooling effect of clouds, since the former is most efficient at strong updrafts, and the latter at lower updraft velocities. The latter mechanism does not seem to substantially increase cloud albedo on its own, but in conjunction with gas-phase heating, can decrease the effects of heating. This means that the mixing state of the BC, i.e., whether it is located in the interstitial aerosol, or included within the cloud droplets, can influence the resulting cloud droplet population and optical properties. For the con-

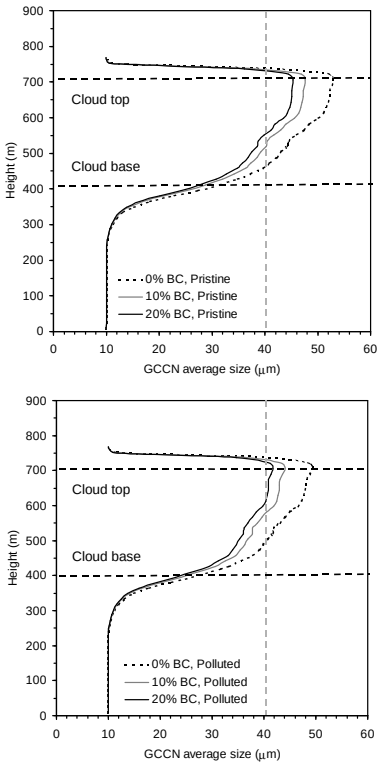

Figure 11. Same as Figure 10, but for a GCCN dry diameter of 10 μm.

ditions studied here, the change in cloud albedo relative to a cloud without radiative heating can be as large as 0.025. The presence of radiative heating seems to decrease cloud albedo; the simulations indicate that this is an effect of decreased LWC; droplet concentrations either remain the same or increase.

The effect of gas-phase heating on the cloud dynamics still remains to be addressed. An immediate effect of the released heat is to increase the buoyancy of the cloud parcel; this would tend to accelerate the cloud parcel, and possibly lead to additional activation of cloud droplets. The former effect is a negative feedback, since the additional activated CCN can enhance cloud albedo. This is an effect relevant for activation timescales ($\sim$ 1 min); for longer timescales however, radiative heating tends to destabilize the stratocumulus cloud layer by decreasing the efficiency of radiative cooling at the top of the cloud layer [*Ackerman et al.*, 2000; *Ackermann and Toon*, 1996]. An appropriate tool for addressing the importance of such feedbacks, is an LES cloud simulation. The importance of these feedbacks on droplet number remains an open question.

The effect of radiative heating on the ability of Giant Cloud Condensation Nuclei (GCCN) to reach sizes that are generally considered necessary to initiate precipitation is examined by assessing the effect of droplet growth kinetics on the size of GCCN using: *i*) adiabatic parcel theory, and, *ii*) trajectories derived from a large eddy simulation of a marine stratocumulus deck. It is shown through theoretical arguments and simulations that radiative heating consistently decreases the size of GCCN, regardless of the GCCN dry size and type of supersaturation profile to which the particle was exposed to. The simulations also suggest that this size reduction can effectively reduce the probability of drizzle formation for both polluted and pristine cloud conditions.

Incorporating the effect of BC on droplet activation in a global model is possible; one needs to account for the gas-phase heating and changes in the CCN spectrum from BC inclusions in a coupled manner. The former can be addressed using an "effective vertical velocity" approach, such as that proposed in *Ghan et al.* [1993]; while the latter can be treated by appropriate modifications to a droplet activation parameterization (illustrated in Part 1). However, this approach, apart from any inherent uncertainties, neglects any subsequent effects on cloud dynamics that arise from the BC heating.

Assessing the global impact of BC on GCCN is not currently possible, although this works suggests that the controlling factors that determine the relative size

reduction from BC heating are the BC content and average updraft velocity. The simulations further indicate that simple adiabatic parcel theory can be used to assess the size reduction for the average vertical velocity of the updrafts, although this is subject to further evaluation.

The simulations presented in this study comprehensively define the effects of BC absorption on cloud formation; however, more work is needed to provide a conclusive assessment. This work does show, however, that effects of BC forcing on climate are more complex than currently thought.

Acknowledgments. This work was supported by Office of Naval Research grant N00014-96-1-0119. The authors would like to thank Dr. Graham Feingold for providing the LES trajectories used in this work, and an anonymous reviewer for helpful comments.

References

Ackerman, A., O. Toon, D. Stevens, A. Heymsfield, V. Ramanathan, and E. Welton, Reduction of tropical cloudiness by soot, *Science*, *288*, 1042–1047, 2000.

Ackermann, A., and O. Toon, Unrealistic dessication of marine stratocumulus clouds by enhanced solar absorption, *Nature*, *380*, 512–515, 1996.

Chýlek, P., G. Lesins, G. Videen, J. Wong, R. Pinnick, D. Ngo, and J. Klett, Black carbon and absorption of solar radiation by clouds, *J. Geophys. Res.*, *101*, 23,365–23,371, 1996.

Feingold, G., W. Cotton, S. Kreidenweis, and J. Davis, The impact of giant cloud condensation nuclei on drizzle formation in stratocumulus: Implications for cloud radiative properties, *J. Aerosol Sci.*, *56*, 4100–4117, 1999.

Fuller, K., W. Malm, and S. Kreidenweis, Effects of mixing on extinction by carbonaceous particles, *J. Geophys. Res.*, *104*, 15,941–15,954, 1999.

Ghan, S., C. Chuang, and J. Penner, A parameterization of cloud droplet nucleation. part i: Single aerosol species, *Atmos. Res.*, *30*, 197–222, 1993.

Ghan, S., G. Guzman, and H. Abdul-Razzak, Competition between sea-salt and sulfate particles as cloud condensation nuclei, *J. Atmos. Sci.*, *55*, 3340–3347, 1998.

Hansen, J., M. Sato, and R. Ruedy, Radiative forcing and climate response, *J. Geophys. Res.*, *102*, 6831–6864, 1997.

Hoppel, W., G. Frick, and J. Fitzgerald, Deducing droplet concentration and supersaturation in marine boundary layer clouds from surface aerosol measurements, *J. Geophys. Res.*, *101*, 26,553–26,565, 1996.

Hudson, J., Effects of CCN concentrations on stratus clouds, *J. Aerosol Sci.*, *40*, 480–486, 1983.

Lacis, A. A., and J. E. Hansen, A parameterization for the absorption of solar radiation in the earth's atmosphere, *J. Aerosol Sci.*, *31*, 118–133, 1974.

Lohmann, U., and J. Feichter, Can the direct and semi-direct aerosol effect compete with the indirect effect on a global scale?, *Geophys. Res. Lett.*, *28*, 159–161, 2001.

Nenes, A., S. Ghan, H. Abdul-Razzak, P. Chuang, and J. Seinfeld, Kinetic limitations on cloud droplet formation and impact on cloud albedo, *Tellus B*, *53*, 133–149, 2001.

Smith, M. H., A. Jones, J. A. Lowe, and C. D. O'Dowd, Role of atmospheric aerosol in the indirect climate cooling mechanism., *12th Int.Conference on Clouds and Precipitation, Zurich*, 1996.

Smolik, J., L. Dzumbova, J. Schwarz, and M. Kulmala, Evaporation of ventilated water droplet: connection between heat and mass transfer, *J. Aerosol Sci.*, *33*, 205–205, 2002.

Stevens, B., G. Feingold, W. Cotton, and R. Walco, Elements of the microphysical structure of numerically simulated nonprecipitating stratocumulus, *J. Aerosol Sci.*, *53*, 980–1006, 1966.

Whitby, K., The physical characteristics of sulfur aerosols, *Atmos. Environ.*, *12*, 135–159, 1978.

A. Nenes, W. C. Conant and J. H. Seinfeld, Department of Chemical Engineering, California Institute of Technology, Pasadena CA, 91125. (e-mail: nenes@caltech.edu; billc@cheme.caltech.edu; seinfeld@caltech.edu)

Received February 27, 2002; revised April 11, 2002; accepted April 15, 2002.